# Synthesis, sensor activity and logic behaviour of a novel bichromophoric system based on rhodamine 6G and 1,8-naphthalimide

**ARTICLE** *in* DYES AND PIGMENTS · APRIL 2015

Impact Factor: 3.97 · DOI: 10.1016/j.dyepig.2015.01.001



**5 AUTHORS**, INCLUDING:

Nikolai I Georgiev
University of Chemical Technology and Met…
**40** PUBLICATIONS **732** CITATIONS
SEE PROFILE

Abdullah M. Asiri
King Abdulaziz University
**1,164** PUBLICATIONS **6,886** CITATIONS
SEE PROFILE

Vladimir Bojinov Bojinov
University of Chemical Technology and Met…
**101** PUBLICATIONS **2,117** CITATIONS
SEE PROFILE

Dyes and Pigments 115 (2015) 172–180

Contents lists available at ScienceDirect

Dyes and Pigments

journal homepage: www.elsevier.com/locate/dyepig

# Synthesis, sensor activity and logic behaviour of a novel bichromophoric system based on rhodamine 6G and 1,8-naphthalimide

Nikolai I. Georgiev [a], Margarita D. Dimitrova [a], Abdullah M. Asiri [b, c], Khalid A. Alamry [b], Vladimir B. Bojinov [a, b, *]

[a] Department of Organic Synthesis, University of Chemical Technology and Metallurgy, 8 Kliment Ohridsky Str., 1756 Sofia, Bulgaria
[b] Chemistry Department, Faculty of Sciences, King Abdulaziz University, P.O. Box 80203, Jeddah 21589, Saudi Arabia
[c] Center of Excellence for Advanced Materials Research (CEAMR), King Abdulaziz University, Jeddah 21589, P.O. Box 80203, Saudi Arabia

ARTICLE INFO

*Article history:*
Received 3 November 2014
Received in revised form
27 December 2014
Accepted 3 January 2015
Available online 9 January 2015

*Keywords:*
1,8-Naphthalimide/Rhodamine 6G conjugate
Fluorescence resonance energy transfer (FRET)
Photoinduced electron transfer (PET)
Internal charge transfer (ICT)
OR and INHIBIT logic gates
Two output combinatorial logic circuit

ABSTRACT

A novel fluorescence sensing system based on rhodamine 6G and 1,8-naphthalimide fluorophores was synthesized and investigated. The system was designed as a wavelength-shifting bichromophoric molecule where the 1,8-naphthalimide moiety is an energy "donor" capable of absorbing light and efficiently transferring the energy to a focal Rhodamine 6G "acceptor". Furthermore, the 1,8-naphthalimide unit was configured on the "*fluorophore-spacer-receptor*" format. Thus, the distinguishing features of fluorescence resonance energy transfer systems were successfully combined with the properties of photoinduced electron transfer and classical ring-opening sensor systems. The synthesized compound shows excellent signalling properties towards protons as well as $Cu^{2+}$ and $Hg^{2+}$ over the representative metal ions. Due to the remarkable fluorescence changes in the presence of protons, $Cu^{2+}$ and $Hg^{2+}$ ions the novel system is able to act as a two output combinatorial logic circuit with three chemical inputs.



## 1. Introduction

Detection of trace amounts of species such as protons and metal ions is of great interest in the fields of chemical, biological, medicinal and environmental sciences [1–6]. In this regard, fluorescence spectroscopy affords an easy way of sensing and imaging cations because of its simplicity and high sensitivity [7–9].

Determination of pH is one of the most important analytical methods in the chemical laboratories and in the industry. pH is a key parameter in clinical analysis, food production, biotechnological processes, waste water treatment procedures, environmental and life sciences [10–16]. Intracellular pH environments play a central modulating role in biosystems, since minor variations in pH may lead to markedly changed cellular behaviour in proliferation, apoptosis, enzymatic activity and ion transport [17,18]. Accordingly, some illnesses like cancer, stroke and Alzheimer's disease are found to be accompanied with pH changes [19,20]. Hence the development of simple and convenient approaches for detecting pH is of great importance in both cellular analysis and diagnosis.

Developing sensors for selective and sensitive detection of mercury species have received an immense interest due to their extreme toxicity towards humans [21,22]. Mercury is the third most frequently found and second most common toxic heavy metal in the list of the Agency for Toxic Substances and Disease Registry (ATSDR) of the U.S. Department of Health and Human Services [23]. The extreme toxicity of mercury and its derivatives results from its high affinity for thiol groups in proteins and enzymes, leading to the dysfunction of cells and consequently causing health problems [24,25]. Unfortunately, mercury contamination can occur through a variety of natural and anthropogenic sources including oceanic and volcanic emissions, gold mining, and combustion of fossil fuels. Thus, the health concerns over exposure to mercury have

* Corresponding author. Department of Organic Synthesis, University of Chemical Technology and Metallurgy, 8 Kliment Ohridsky Str., 1756 Sofia, Bulgaria. Tel.: +359 2 8163206.
*E-mail address:* vlbojin@uctm.edu (V.B. Bojinov).

http://dx.doi.org/10.1016/j.dyepig.2015.01.001
0143-7208/

motivated the exploration of selective and efficient methods for the monitoring of mercury in biological and environmental samples.

Rhodamine fluorophore has consistently demonstrated its potential to construct fluorescent sensors for determination of protons and mercury, ascribing to their spirolactam ring-opening equilibrium [26–30]. The single emission-based probes usually tend to be affected by a variety of factors such as instrumental efficiency and environmental conditions, as well as the concentration of the probe molecule. These interferences can be eliminated by employing ratiometric fluorescent probes, which allow the measurement of changes of the intensity ratio at two emission bands to provide built-in correction for the above-mentioned environmental effects [9,25,27,31,32]. Several strategies, including internal charge transfer (ICT) [33,34], excited-state intramolecular proton transfer (ESIPT) [35] and fluorescence resonance energy transfer (FRET) [36,37], have been adopted to design ratiometric probes. Among them, FRET strategy could provide moderate resolution of the two emission bands and has been widely applied in designing ratiometric probes for bioanalyitcal applications. In this work, a novel ratiometric fluorescent probe for pH and mercury detection was developed combining the advantages of the FRET based bichromophoric systems and Rhodamine receptor abilities.

Since the first suggestion for Boolean operator at molecular level based on fluorescent chemosensors, the field has rapidly extended from simple switches to more complex molecular systems that are capable of performing a variety of classical logic functions [38–40] and examples of half-adder [41,42], full-adder [43], keypad lock [44], half-subtractor [45], full-subtractor [43], encoder-decoder [46] and a digital comparator [47–49] have been described. Also a smart oligonucleotide-based automaton that plays simple games such as Tic-Tac-Toe have been reported [50]. Such logic functions are of elevated interest for applications such as object coding, intelligent materials, drug delivery and activation, diagnostics or actuation [51,52]. Nevertheless, the physical integration of molecular logic gates is especially important for rational design and implementation towards advanced molecular scale computing. Herein, we propose a cascade of two molecular fluorescent chemosensors that are integrated in logic circuit comprising a FRET bichromophoric system. The examined bichromophoric system was constructed by coupling of a Rhodamine 6G acceptor dye and a photoinduced electron transfer (PET) based 1,8-naphthalimide donor (Scheme 1).

## 2. Experimental

### 2.1. Materials

The intermediate compounds **2** and **3** were prepared according to the reported procedure [53]. Commercially available ethylenediamine and methylacrylate (Aldrich) were used without purification. All solvents (Aldrich, Fisher Chemical) were pure or of spectroscopy grade. Commercial aqueous buffer solution HEPES (Fisher Chemical) was used as received. $Zn(NO_3)_2$, $Cu(NO_3)_2$, $Ni(NO_3)_2$, $Co(NO_3)_2$, $Pb(NO_3)_2$, $Fe(NO_3)_3$, $Hg(NO_3)_2$, and $AgNO_3$ salts were the sources for metal cations (all Aldrich salts at p.a. grade).

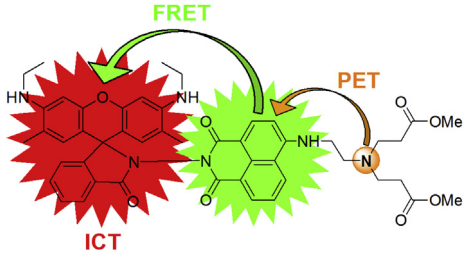


**Scheme 1.** Rhodamine 6G/1,8-naphthalimide wavelength-shifting bichromophoric system.

### 2.2. Methods

FT-IR spectra were recorded on a Varian Scimitar 1000 spectrometer. The $^1$H NMR spectra (chemical shifts are given in ppm) were recorded on a Bruker DRX-250 spectrometer operating at 250.13 MHz. TLC was performed on silica gel, Fluka F60 254, 20 × 20, 0.2 mm. The melting points were determined by means of a Kofler melting point microscope. The UV–VIS absorption spectra were recorded on a spectrophotometer Hewlett Packard 8452A. The fluorescence spectra were taken on a Scinco FS-2 spectrofluorimeter. The fluorescence quantum yields ($\Phi_F$) were measured relatively to Rhodamine 6G ($\Phi_F = 0.95$ in ethanol [54]) or Coumarin 6 ($\Phi_F = 0.78$ in ethanol [55]) as standards. All the experiments were performed at room temperature (25.0 °C). A 1 × 1 cm quartz cuvette was used for all spectroscopic analysis. To adjust the pH, very small volumes of hydrochloric acid and sodium hydroxide were used. The effect of the metal cations upon the fluorescence intensity was examined by adding portions of the metal cations stock solution to a known volume of the fluorophore solution (10 mL). The addition was limited to 100 μL so that dilution remains insignificant.

### 2.3. Synthesis of dyad (*4*)

To a solution of **3** (1.96 g, 3 mmol) in DMF (30 mL), ethylenediamine (6.2 mL, 30 equiv. per reactive nitro group) was added at room temperature. After 48 h, the resulting solution was poured into water. The precipitate was filtered off and washed with water. The final product **4** was obtained as yellow solid after purification by column chromatography using silica gel as a stationary phase and methanol/ammonium hydroxide = 5:0.4 as eluent. In order to remove the silica gel particles, the solid was dissolved in chloroform, resulting solution was filtrated off and the solvent was evaporated in vacuum.

Yield: 1.24 g (62%), m.p. > 250 °C, $R_f = 0.48$ (methanol/ammonium hydroxide = 5:0.4) IR (KBr) cm$^{-1}$: 3313 and 3224 (νNH and $\nu NH_2$); 2927 and 2885 (νCH); 1706 ($\nu^{as}$N-C=O); 1674 ($\nu^{s}$N-C=O). $^1$H NMR ($CDCl_3$-*d*, 250.13 MHz) ppm: 8.18 (d, 1H, $J$ = 8.4 Hz, Naphthalimide H-7); 8.11 (m, 1H, 9-Ph H-3); 7.73 (d, 1H, $J$ = 8.6 Hz, Naphthalimide H-2); 7.65 (m, 2H, 9-Ph H-4, 9-Ph H-5); 7.56 (d, 1H, $J$ = 7.2 Hz, Naphthalimide H-5); 7.29 (m, 1H, 9-Ph H-6); 7.00 (dd, 1H, $J$ = 8.4, Hz, $J$ = 7.2 Hz, Naphthalimide H-6); 6.51 (m, 3H, Rhodamine H-4, Rhodamine H-5, Naphthalimide 4-NH); 6.21 (d, 1H, $J$ = 8.6 Hz, Naphthalimide H-3); 6.05 (s, 1H, Rhodamine H-1); 6.00 (s, 1H, Rhodamine H-8); 3.41 (br.s, 2H, 2 × NH); 3.22 (m, 2H, $NHCH_2CH_2NH_2$); 3.03 (m, 6H, $NHCH_2CH_2NH_2$, Rhodamine 2 × $CH_2CH_3$); 1.98 (s, 3H, Rhodamine $CH_3$); 1.97 (s, 3H, Rhodamine $CH_3$); 1.20 (m, 8H, $NH_2$, Rhodamine 2 × $CH_2CH_3$). Elemental analysis: Calculated for $C_{40}H_{38}N_6O_4$ (MW 666,8) C 72.05, H 5.74, N 12.60%; Found C 72.31, H 5.85, N 12.44%.

### 2.4. Synthesis of dyad (*5*)

A suspension of Dyad **4** (1.0 g, 1.5 mmol) in methanol (20 mL) was added dropwise over period of 20–30 min to a solution of methylacrylate (1.4 mL, 10 equiv. per reactive amine group) in 2 mL of cooled to 0 °C methanol. The reaction was allowed to warm slowly to room temperature and then stirred for 3 days. The final product was obtained as yellow solid after purification by column chromatography using silica gel as a stationary phase and toluene/ethyl acetate/ethanol = 3:3:1 as eluent. In order to remove the silica

gel particles, the solid was dissolved in chloroform, resulting solution was filtrated off and the solvent was evaporated in vacuum.

Yield: 0.91 g (73%), m.p 194–195 °C, $R_f$ = 0.74 (toluene/ethyl acetate/ethanol = 3:3:1). IR (KBr) $cm^{-1}$: 3366 (νNH); 2921 and 2878 (νCH); 1722 (νC = OOMe); 1676 (νN-C=O). $^1$H NMR ($CDCl_3$-*d*, 250.13 MHz) ppm: 8.26 (d, 1H, *J* = 8.3 Hz, Naphthalimide H-7); 8.11 (m, 3H, 9-Ph H-3, 9-Ph H-4 и Naphthalimide H-2); 7.64 (m, 2H, 9-Ph H-5, Naphthalimide H-5); 7.40 (t, 1H, *J* = 7.9 Hz, Naphthalimide H-6); 7.30 (m, 1H, 9-Ph H-6); 6.61 (m, 2H, Rhodamine H-4, Rhodamine H-5); 6.47 (d, 1H, *J* = 8.5 Hz, Naphthalimide H-3); 6.21 (br.s, 1H, Naphthalimide NH); 6.12 (s, 1H, Rhodamine H-1); 6.10 (s, 1H, Rhodamine H-8); 3.59 (s, 6H, 2 × $CH_2OOCH_3$); 3.45 (br.s, 2H, 2 × NH); 3.22 (m, 2H, $NHCH_2CH_2$); 3.03 (m, 4H, Rhodamine 2 × $CH_2CH_3$); 2.86 (t, 6H, *J* = 6.3 Hz, 3 × $NCH_2$); 2.51 (t, 4H, *J* = 6.4 Hz, 2 × $CH_2COOCH_3$); 2.03 (s, 6H, 2 × Rhodamine $CH_3$); 1.20 (m, 6H, Rhodamine 2 × $CH_2CH_3$). Elemental analysis: Calculated for $C_{48}H_{50}N_6O_8$ (MW 839,0) C 68.72, H 6.01, N 10.02%; Found C 69.08, H 6.17, N 9.77%.

## 3. Results and discussion

### 3.1. Design and synthesis

It is well known that the spectral overlap between the emission of the donor fluorophore and the absorbance of the acceptor is the main factor that determines the efficiency of FRET systems [56]. When constructing the novel FRET system **5**, the 4-amino-1,8-naphthalimide fluorophore was chosen as an energy donor due to its strong emission in the visible region (450–600 nm) which covers a part of rhodamine absorption, thus providing favourable conditions for the FRET process [57,58]. Also, the 1,8-naphthalimide donor is a PET based chemosensing system with a diester terminated amine receptor [59]. Thus we expect that the PET process in 1,8-naphthalimide will effectively quench the fluorescence of the yellow-green emitting donor and affect the FRET efficiency to the rhodamine unit, which represents the "*off-state*" of the system. Coupling the amine receptor with the analyte (protons or different metal ions) would increase its oxidation potential, and as such, thermodynamically disallow the electron transfer to the donating 1,8-naphthalimide. Consequently the energy transfer to the acceptor would be "*switched on*" (Scheme 2).

The synthesis of the desired wavelength-shifting bichromophore **5** was accomplished in four steps as outlined in Scheme 3.

First, intermediate **3** was obtained as we previously reported by condensation of Rhodamine 6G hydrazide **2** with 4-nitro-1,8-naphthalic anhydride in glacial acetic acid at 110 °C for 5 h. Rhodamine 6G hydrazide **2** was obtained by reaction of Rhodamine 6G **1** with hydrazine monohydrate under reflux in absolute ethyl alcohol for 5 h [53].

Thus prepared intermediate **3** was nucleophilically substituted with the commercially available ethylenediamine in DMF solution at room temperature for 48 h. Finally, the reaction of intermediate **4** with methylacrylate in methanol gave the novel Dyad **5**.

The synthesized compounds were characterized by their melting points and TLC retention values ($R_f$) and identified by conventional techniques - elemental analysis data, UV–Vis, fluorescence, FT-IR and $^1$H NMR spectroscopy.

For instance, in the $^1$H NMR ($CDCl_3$-*d*, 250.13 MHz) spectrum of Dyad **4** a resonance at 6.21 ppm (Fig. 1a, **I**) was observed which is characteristic for the proton in position C-3 of the yellow-green emitting 1,8-naphthalimide, substituted in position C-4 with an electron-donating amino group. This resonance is different from the corresponding resonance for the 4-nitro-1,8-naphthalimide moiety in intermediate **3** (8.35 ppm) [53]. This is solid evidence that the 4-nitro-1,8-naphthalimide unit in **3** was completely converted into the yellow-green emitting donor fluorophore (Dyad **4**). Furthermore, in the $^1$H NMR spectrum of final Dyad **5** a singlet at 3.59 ppm for 6 protons (Fig. 1b, **II**) and two triplets at 2.86 ppm for 6 protons (Fig. 1b, **III**) and at 2.51 ppm for 4 protons (Fig. 1b, **IV**) appeared which is typical for the desired diester terminated receptor unit [60] suggesting that the starting primary amine in Dyad **4** was successfully branched to give the diester moiety in Dyad **5**.

### 3.2. Influence of pH on the photophysical properties of dyad *5*

Photophysical properties of Dyad **5** were determined in water/acetonitrile (4:1, v/v) solution. In alkaline and neutral media (pH > 6) the rhodamine moiety adopts a closed, non-fluorescent spirolactam form. This results in absorption of the system at about 420–440 nm, which is attributed to an internal charge transfer process in the 1,8-naphthalimide chromophore. At *ca*. pH 5 the spirolactam ring of rhodamine is opened and a new absorption (rhodamine) band with well pronounced maximum at 530 nm appears (Fig. 2) which gradually increases upon increasing the acidity of solution up to pH 2. Also, a blue shift of the 1,8-naphthalimide absorption band ($\Delta\lambda_A$ = 13 nm) in acid media was observed (Fig. 2). This effect probably is due to protonation of the amine receptor of compound **5** that give rise to some weak charge repulsion on the aromatic amine of the donor fluorophore, which is well correlated with the data for the 1,8-naphthalimide derivatives [61–63].

From the absorption changes at 530 nm, the titration curve of novel compound was obtained. The analysis of the titration plot according to Eq. (1) [64] gives the p$K_a$ value of 4.7, which is similar to the other rhodamine derivatives [65].

$$\log[(A_{max} - A)/A - A_{min}] = pH - pK_a \quad (1)$$

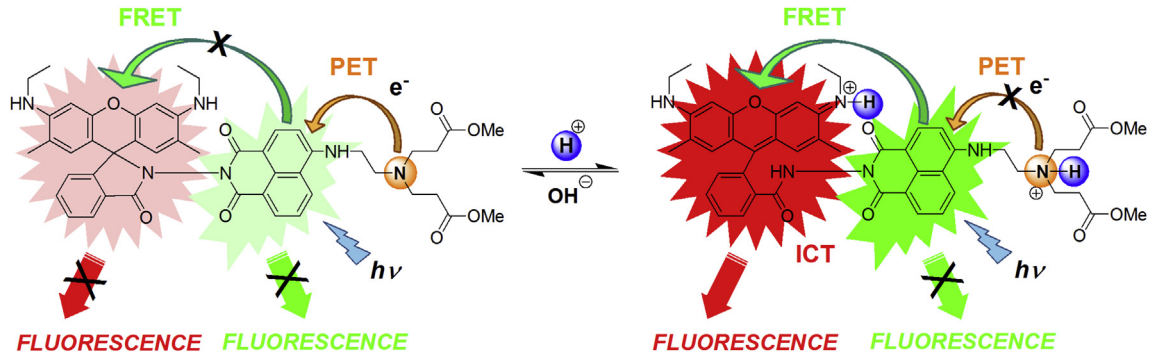


**Scheme 2.** Photophysical behaviour of bichromophoric system **5** as a function of pH after excitation within a spectral region of maximal absorption of the donating fluorophore.

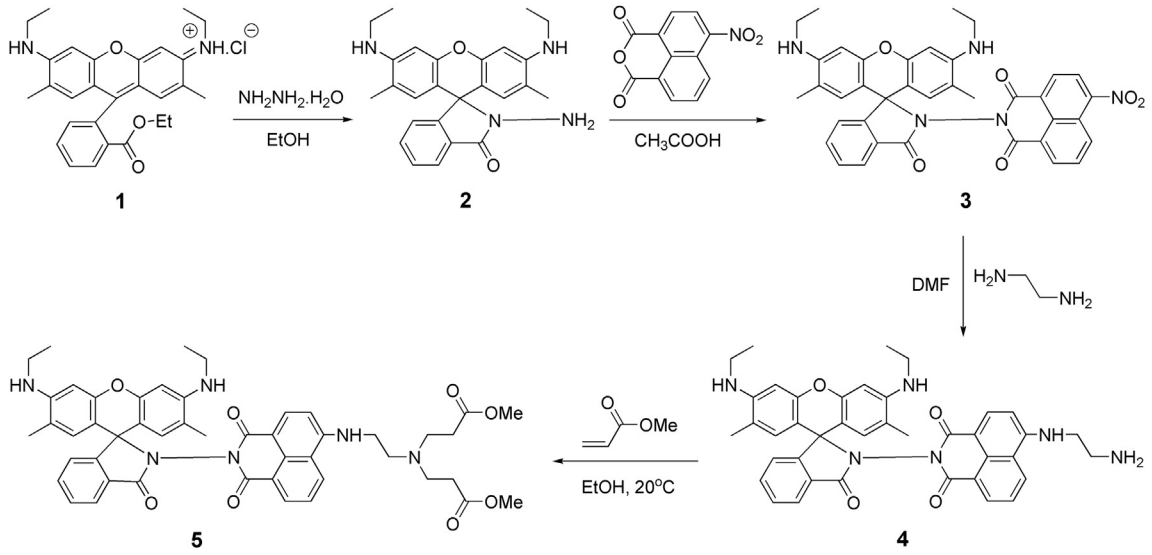


**Scheme 3.** Synthesis of wavelength-shifting bichromophoric system **5**.

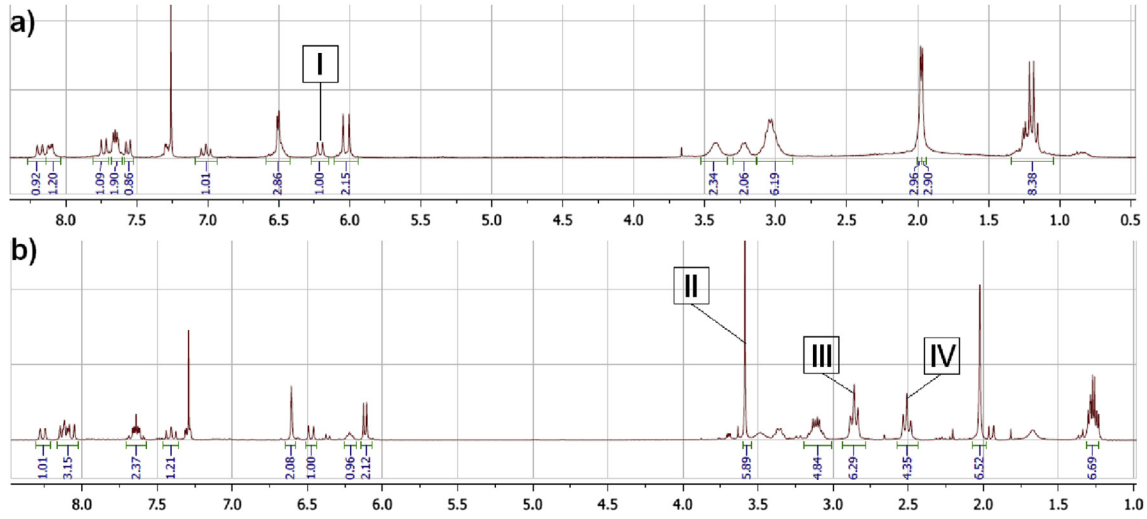


**Fig. 1.** $^1$H NMR ($CDCl_3$-*d*, 250.13 MHz) spectra of Dyad **4** (a) and Dyad **5** (b).

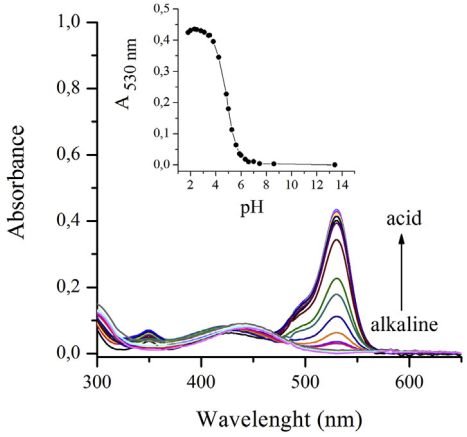


**Fig. 2.** Effect of pH on the UV/Vis absorption spectra of Dyad **5**. Inset: Titration plot of Dyad **5** at $\lambda_A = 530$ nm in a pH range of *ca.* 13–2.

In alkaline and neutral media, after excitation at 420 nm (within the spectral region of maximal absorption of the donor fluorophore) the novel fluorescence probe shows only week emission in the range of 480–700 nm with maximum at 539 nm. Under these conditions, the acceptor dye is in a spirolactam form and energy transfer from the donor fluorophore to the rhodamine is not possible. In this case the system shows a yellow-green emission that is typical for the 4-amino-1,8-naphthalimide derivatives. The quantum yield of fluorescence in water/acetonitrile (4:1, v/v) solution was calculated using Coumarin 6 ($\Phi_F = 0.78$ in ethanol [55]) as a standard according to Eq. (2) [66], where $A_{ref}$, $S_{ref}$, $n_{ref}$ and $A_{sample}$ $S_{sample}$, $n_{sample}$ represent the absorbance at the exited wavelength, the integrated emission band area and the solvent refractive index of the standard and the sample, respectively.

$$\Phi_F = \Phi_{ref}\left(\frac{S_{sample}}{S_{ref}}\right)\left(\frac{A_{ref}}{A_{sample}}\right)\left(\frac{n^2_{sample}}{n^2_{ref}}\right) \quad (2)$$

However, the calculated quantum yield of Dyad **5** at pH 7 was 0.02 which is extremely low compared to the quantum yield of the

traditional 4-amino-1,8-naphthalimides, not containing an amine receptor [59]. This phenomenon might be caused by the possible photoinduced electron transfer from the alkylamino receptor to the 4-amino-1,8-naphthalimide fluorophore. Thus the fluorescence of the 4-amino-1,8-naphthalimide fluorophore is quenched (Scheme 2). It is also worth noting that the calculated quantum yield of Dyad **5** water/acetonitrile (4:1, v/v) was even lower than the quantum yield of 1,8-naphthalimide fluorophores with a receptor fragment. The reason for such behaviour of the novel compound could be twofold: (i) It is well known that the water is an effective fluorescence quencher, which additionally decreased the quantum yield in the aqueous medium; (ii) Novel Dyad **5** is highly hydrophobic and probably quenches its emission in the aqueous solution due to the aggregation process.

The used diester terminated naphthalimide acceptor shows p$K_a$ value of about 4.8 [59]. Upon acidification from pH 6 to 2, the tertiary amine receptor is protonated which prevents the PET quenching process in the donor 1,8-naphthalimide. Nevertheless, the 1,8-naphthalimide emission does not increase because the spirolactam ring becomes open under these conditions, which allows the energy transfer to the rhodamine acceptor moiety. This results in remarkable fluorescence intensity enhancement (FE = 358) in the rhodamine emission region at 555 nm (Fig. 3). The quantum yield of fluorescence of rhodamine moiety in Dyad **5** ($\lambda_{ex}$ = 510 nm) was calculated to be $\Phi_F$ = 0.27 at pH 2 in water/acetonitrile (4:1, v/v) using Rhodamine 6G ($\Phi_F$ = 0.95 in ethanol [54]) as a standard.

The analysis of the fluorescence changes at 555 nm (Fig. 3) according to Eq. (3) [64] gives the p$K_a$ value of 4.6 which is very similar to the p$K_a$ value calculated according absorption changes and is attributed to the spirolactam ring-opening reaction.

$$\log[(I_{F\,max} - I_F)/I_F - I_{F\,min}] = pH - pK_a \quad (3)$$

### 3.3. Influence of metal cations on the fluorescence intensity of dyad **5**

The signalling fluorescent properties of Dyad **5** in the presence of transition metal cations ($Co^{2+}$, $Cu^{2+}$, $Fe^{3+}$, $Ni^{2+}$, $Pb^{2+}$, $Zn^{2+}$, $Hg^{2+}$ and $Ag^{+}$) were investigated in acetonitrile. For a constant pH, the solutions were buffered with addition of 1 mmol HEPES solution (pH = 7.2). The HEPES buffer was chosen because it ensures a pH value about pH = 7 where the PET based 1,8-naphthalimide donor and rhodamine acceptor units in Dyad **5** are in their *"off-state"* and cation recognition in the both moieties is feasible. The changes in the fluorescence spectrum of bichromophoric system observed after addition of 10 equivalents of examined metal ions are presented in Fig. 4. As can be seen, only $Cu^{2+}$ and $Hg^{2+}$ remarkably affected the fluorescence spectrum of Dyad **5**. The $Cu^{2+}$ ions increased the fluorescence intensity of naphthalimide donor, while the presence of $Hg^{2+}$ ions resulted in a strong fluorescence enhancement of the rhodamine acceptor. Although a fluorescence enhancement of rhodamine unit in Dyad **5** was occurred when $Pb^{2+}$ was added, this effect is negligible compared with the influence of $Hg^{2+}$ and do not affect naphthalimide fluorescence output. This suggests that the ability of Dyad **5** to bind $Pb^{2+}$ ions is a very low.

Upon addition of $Cu^{2+}$ a fluorescence enhancement of the 1,8-naphthalimide donor emission in dyad **5** was observed (Fig. 5A). Obviously, among the examined metal cations only $Cu^{2+}$ is able to bind the PET amine receptor of the 1,8-naphthalimide unit. Upon recognition of $Cu^{2+}$, which binds the 1,8-naphthalimide receptor engaging its lone-pair electrons, the PET process is no longer possible and the 1,8-naphthalimide fluorescence is increased. The enhancement of the fluorescence emission (FE) has been used as a qualitative parameter. The FE = $I/I_o$ is determined as the ratio between the maximum fluorescence intensity ($I$ - after metal ion addition) and the minimum fluorescence intensity ($I_o$ - free of metal cations solution). The calculated FE value of 2.2 is consistent with the data for a naphthalimide diester of similar nature that was developed before [59]. The stoichiometry of the complex between $Cu^{2+}$ cation and Dyad **5** was determined using the method of continuous variations (Job's method). Job's plot analysis of the titration revealed a maximum at about 0.5 mol fraction, indicating 1:1 binding stoichiometry (Fig. 5B).

The linear range of the method was found to be at least 2–10 μM $Cu^{2+}$ with a correlation coefficient of $R^2$ = 0.99301. The limit of detection (LOD) was calculated to be $5 \times 10^{-7}$ mol $L^{-1}$ according to formula LOD = 3σ/b where σ is the standard deviation and b is the slope of the calibration plot (Fig. 5A, Inset) [67]. The fluorescence intensity of Dyad **5** without $Cu^{2+}$ was measured by 10 times and the standard deviation of measurements was determined.

In contrast with the effect of $Cu^{2+}$, the addition of $Hg^{2+}$ decreased the 1,8-naphthalimide emission and a new emission band centered at 555 nm (emission of rhodamine acceptor moiety) appeared (Fig. 6A). This fact is solid evidence that the FRET process in Dyad **5** is *"switched on"* by $Hg^{2+}$ ions because the excitation of 1,8-naphthalimide at 420 nm results in emission of the rhodamine

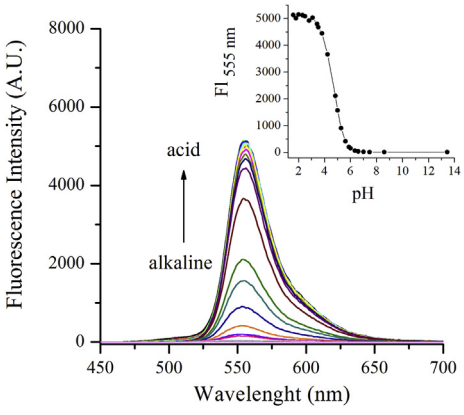


**Fig. 3.** Effect of pH on the fluorescence spectra of Dyad **5**, excited at 420 nm. Inset: Titration plot of Dyad **5** at $\lambda_F$ = 530 nm in a pH range of *ca.* 13–2.

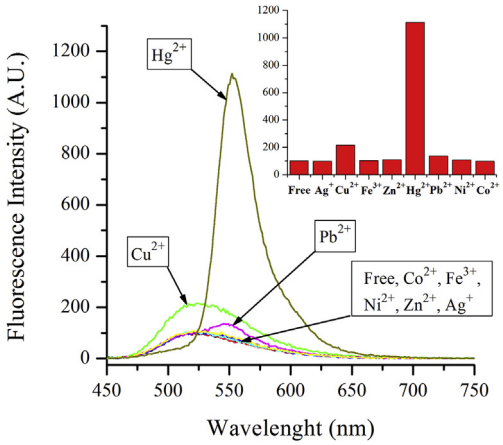


**Fig. 4.** Effect of the metal cations at concentration C = $10^{-4}$ mol $L^{-1}$ on the fluorescence of Dyad **5** (C = $10^{-5}$ mol $L^{-1}$) in acetonitrile solution buffered with 1 mmol HEPES.

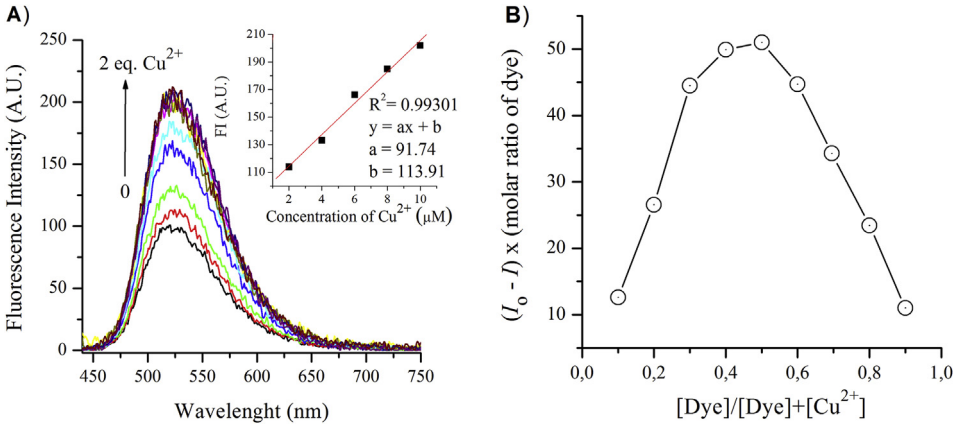


**Fig. 5.** (A) Effect of $Cu^{2+}$ on the fluorescence of Dyad **5** ($C = 10^{-5}$ mol $L^{-1}$) and (B) Job's plot in acetonitrile solution buffered with 1 mmol HEPES. Inset: Calibration plot of Dyad **5**/$Cu^{2+}$.

unit with a maximum at 555 nm. Obviously the $Hg^{2+}$ binds the spirolactam receptor moiety and the rhodamine acceptor of Dyad **5** is converted into the fluorescent ring-opened form. The unique selectivity for $Hg^{2+}$ is probably due to the cooperation of several combined influences, such as the suitable coordination geometry, the proper radius and charge density around oxygen atom of the rhodamine carbonyl group, which takes part in the complexation with the $Hg^{2+}$ ion [68,69]. Also it was found that the rhodamine emission peak at 555 nm attained saturation upon addition of 50 eq. of $Hg^{2+}$. Furthermore the Job's plot analysis (Fig. 6B) revealed 1:1 binding stoichiometry (maximum at about 0.5 mol fraction) suggesting that the $Hg^{2+}$ binding process occurs only in spirolactam receptor fragment in the novel Dyad **5**. The linear range of the method was found to be at least 2–10 μM $Hg^{2+}$ with a correlation coefficient $R^2 = 0.99959$. From the calibration plot (Fig. 6A, Inset) the LOD was calculated to be $9 \times 10^{-8}$ mol $L^{-1}$.

### 3.4. Logic behaviour of dyad *5*

Due to the remarkable fluorescence changes of Dyad **5** (1 eq., $C = 10^{-5}$ mol $L^{-1}$) in the presence of 2 eq. of protons (HCl, $C = 2 \times 10^{-5}$ mol $L^{-1}$), 1 eq. of $Cu^{2+}$ ($C = 10^{-5}$ mol $L^{-1}$) and 1 eq. of $Hg^{2+}$ ($C = 10^{-5}$ mol $L^{-1}$) it would be able to act as a two output combinatorial logic circuit with three chemical inputs. By monitoring the donor emission in Dyad **5** (Output 1, 1,8-naphthalimide fluorescence at 515 nm) a high (coded in binary as 1) fluorescence output was observed only in the presence of $Cu^{2+}$ which cuts off the PET process in the 1,8-naphthalimide fluorophore (Scheme 4). In the presence of protons or $Hg^{2+}$ the rhodamine spirolactam cycle is opened which allows the energy transfer from the 1,8-naphthalimide donor to the rhodamine acceptor, thus quenching the 1,8-naphthalimide emission and preventing the action of $Cu^{2+}$.

So, the fluorescence of 1,8-naphthalimide moiety in the Dyad **5** at 515 nm (Output 1) is high (Fig. 7A, Table 1) only in the presence of $Cu^{2+}$ (Input 3) and in the absence of $Hg^{2+}$ (Input 1) and protons (Input 2) which is correlated very well with a Three-input Disabled INHIBIT gate [70].

By monitoring the rhodamine emission (Output 2, fluorescence at 550 nm), actually, Dyad **5** works as a two input logic gate because $Cu^{2+}$ (Input 3) does not affect by any way the spirolactam opening reaction which is responsible for the high output value (strong emission). In the presence of 1 eq. $Hg^{2+}$ (Input 1) and/or 2 μL 10% HCl (Input 2) a strong emission at 550 nm was observed owning to the spirolactam opened form (Fig. 8, Table 1). This behaviour correlates very well with OR logic gate [70]. The output is high if either or both of the input values are high. If both inputs are low, then the output is low.

On the basis of the present study and results obtained the logic behaviour of Dyad **5** could be summarized with the electronic representation in Scheme 5.

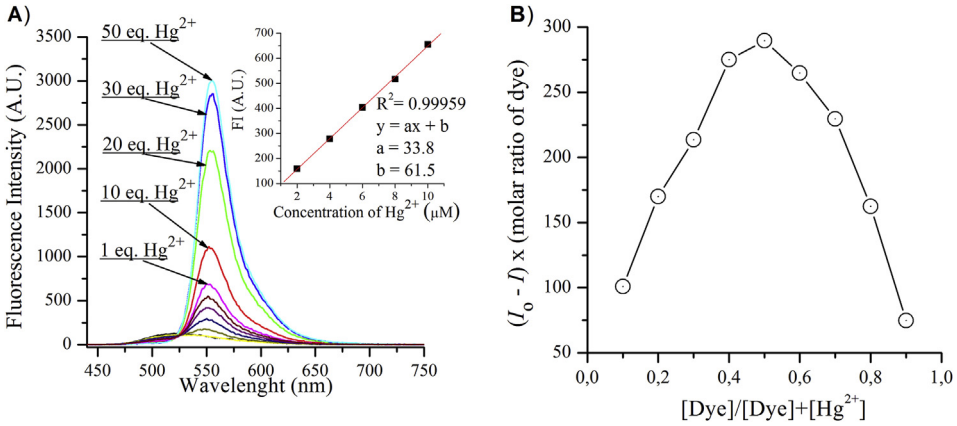


**Fig. 6.** (A) Effect of $Hg^{2+}$ on the fluorescence of Dyad **5** ($C = 10^{-5}$ mol $L^{-1}$) and (B) Job's plot in acetonitrile solution buffered with 1 mmol HEPES. Inset: Calibration plot of Dyad **5**/$Hg^{2+}$.

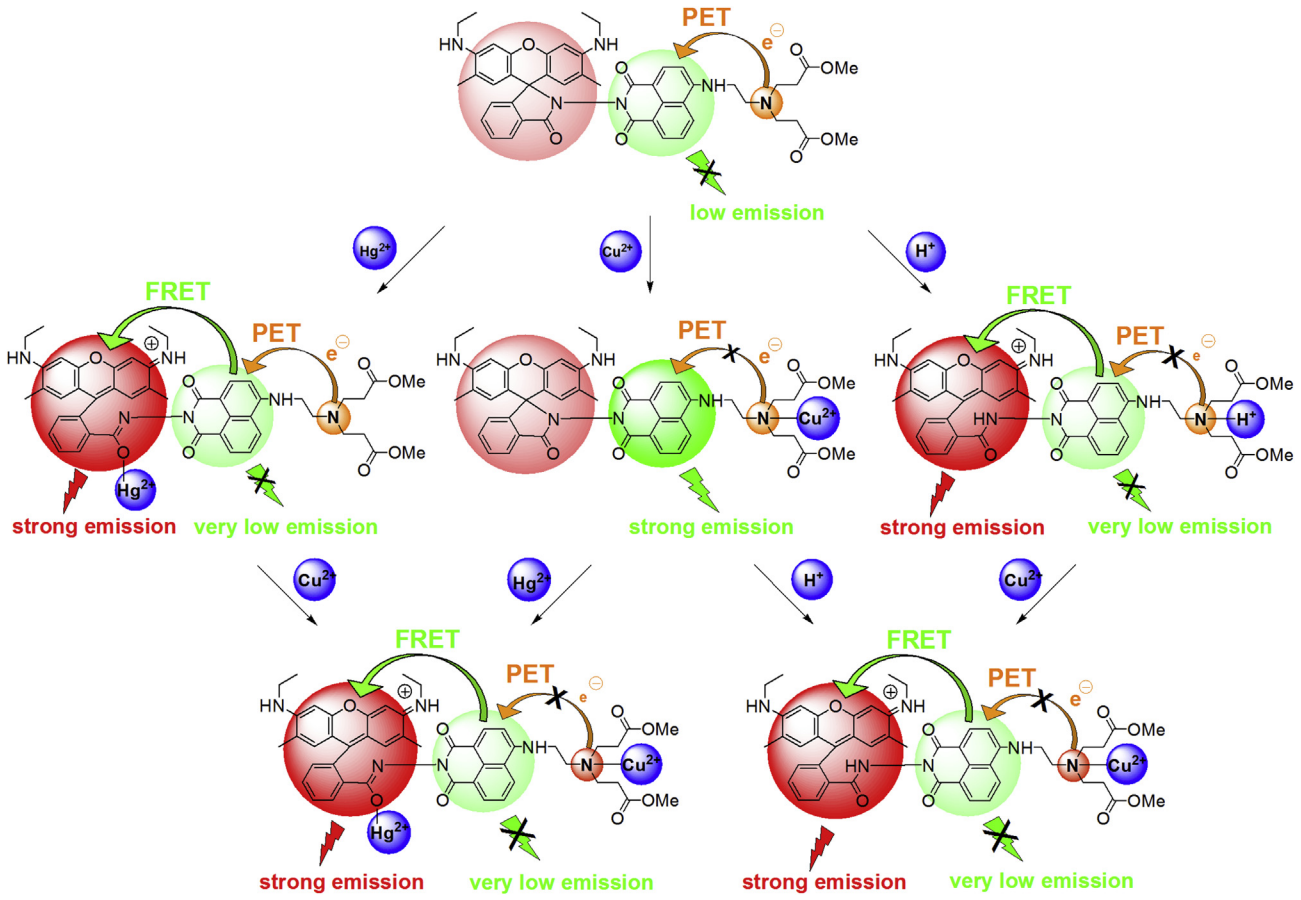


**Scheme 4.** Fluorescence changes of Dyad **5** (1 eq., C = $10^{-5}$ mol $L^{-1}$) in presence of 2 eq. of protons (C = 2 × $10^{-5}$ mol $L^{-1}$), 1 eq. of $Cu^{2+}$ (C = $10^{-5}$ mol $L^{-1}$) and 1 eq. of $Hg^{2+}$ (C = $10^{-5}$ mol $L^{-1}$).

## 4. Conclusions

A novel fluorescent wavelength-shifting bichromophoric system with sensing properties based on FRET, PET and ICT, containing yellow-green emitting 1,8-naphthalimide donor and orange-red emitting rhodamine acceptor, was synthesized and its photophysical behaviour in presence of protons and representative metal ions was studied. The donating 1,8-naphthalimide unit was also designed according to the "*fluorophore-spacer-receptor*" model and as such it would be able to act as a fluorescence PET based chemosensor. In alkaline and neutral media, after excitation within the spectral region of maximal absorption of the donor fluorophore the novel fluorescence probe shows only week yellow-green emission, typical for the 1,8-naphthalimides. Acidification from pH 5 to 2 prevents the PET quenching process in the donor unit and opens the rhodamine spirolactam ring, which allows the energy transfer to the rhodamine acceptor moiety with remarkable fluorescence intensity enhancement (FE = 358) in the rhodamine emission region. In the presence of representative metal ions only $Cu^{2+}$ and $Hg^{2+}$ remarkably affect the fluorescence spectrum of the system. It is shown that only $Cu^{2+}$ is able to bind the amine receptor of the 1,8-naphthalimide unit (1:1 binding stoichiometry), thus preventing the PET process in the donor unit. In contrast, the $Hg^{2+}$

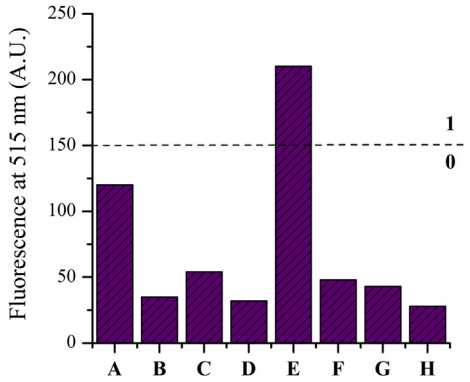


**Fig. 7.** The changes in fluorescence intensity of Dyad **5** (C = $10^{-5}$ mol $L^{-1}$) at 515 nm with 2 eq. of protons (C = 2 × $10^{-5}$ mol $L^{-1}$), 1 eq. of $Cu^{2+}$ (C = $10^{-5}$ mol $L^{-1}$) and 1 eq. of $Hg^{2+}$ (C = $10^{-5}$ mol $L^{-1}$) as chemical inputs.

**Table 1**
The truth table for the operation of 1 eq. of Dyad **5** (C = $10^{-5}$ mol $L^{-1}$) and 2 eq. of protons (C = 2 × $10^{-5}$ mol $L^{-1}$), 1 eq. of $Cu^{2+}$ (C = $10^{-5}$ mol $L^{-1}$) and 1 eq. of $Hg^{2+}$ (C = $10^{-5}$ mol $L^{-1}$) as chemical inputs.

| | Input $Hg^{2+}$ | Input $H^+$ | Input $Cu^{2+}$ | Output Fl $_{515}$ | Output Fl $_{550}$ |
|---|---|---|---|---|---|
| **A** | 0 | 0 | 0 | 0 | 0 |
| **B** | 0 | 1 | 0 | 0 | 1 |
| **C** | 1 | 0 | 0 | 0 | 1 |
| **D** | 1 | 1 | 0 | 0 | 1 |
| **E** | 0 | 0 | 1 | 1 | 0 |
| **F** | 0 | 1 | 1 | 0 | 1 |
| **G** | 1 | 0 | 1 | 0 | 1 |
| **H** | 1 | 1 | 1 | 0 | 1 |

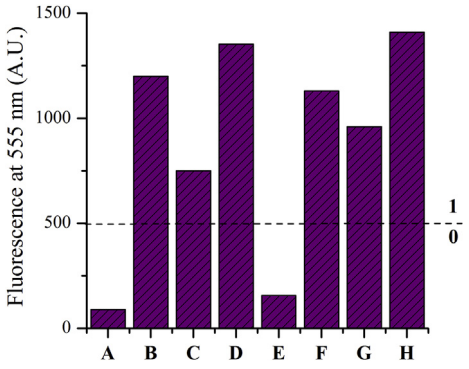


**Fig. 8.** The changes in fluorescence intensity of Dyad **5** ($C = 10^{-5}$ mol $L^{-1}$) at 555 nm with 2 eq. of protons ($C = 2 \times 10^{-5}$ mol $L^{-1}$), 1 eq. $Cu^{2+}$ ($C = 10^{-5}$ mol $L^{-1}$) and 1 eq. $Hg^{2+}$ ($C = 10^{-5}$ mol $L^{-1}$) as chemical inputs.

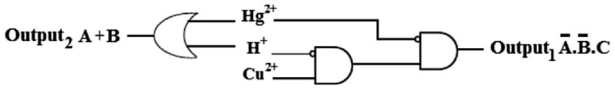


**Scheme 5.** Combinatorial logic circuits on the basis of 1 eq. of Dyad **5** ($C = 10^{-5}$ mol $L^{-1}$) and 2 eq. of protons ($C = 2 \times 10^{-5}$ mol $L^{-1}$), 1 eq. of $Cu^{2+}$ ($C = 10^{-5}$ mol $L^{-1}$) and 1 eq. of $Hg^{2+}$ ($C = 10^{-5}$ mol $L^{-1}$) as chemical inputs.

binding process occurs only in the receptor unit (1:1 binding stoichiometry), which opens the rhodamine spirolactam ring and allows energy transfer to the rhodamine moiety. Due to the remarkable fluorescence changes in the presence of protons, $Cu^{2+}$ and $Hg^{2+}$ ions the novel system is able to execute OR and INHIBIT logic gates and to act as a two output combinatorial logic circuit with three chemical inputs.

## Acknowledgements

This work was supported by the National Science Foundation of Bulgaria (project DDVU-02/97). Authors also acknowledge the Science Foundation at the University of Chemical Technology and Metallurgy (Sofia, Bulgaria).

## References

[1] Chen X, Pradhan T, Wang F, Kim J, Yoon J. Fluorescent chemosensors based on spiroring-opening of xanthenes and related derivatives. Chem Rev 2012;112:1910–56.
[2] Zhang G, Wen Y, Guo C, Xu J, Lu B, Duan X, et al. A cost-effective and practical polybenzanthrone-based fluorescent sensor for efficient determination of palladium (II) ion and its application in agricultural crops and environment. Anal Chim Acta 2013;805:87–94.
[3] Georgiev N, Bryaskova R, Tzoneva R, Ugrinova I, Detrembleur C, Miloshev S, et al. A novel pH sensitive water soluble fluorescent nanomicellar sensor for potential biomedical applications. Bioorg Med Chem 2013;21:6292–302.
[4] Sun Y, Liang X, Zhao Y, Fan J. Studies on the aggregation-induced synchronous emission of 1,8-naphthalimide derivative to casein and its analytic application. Food Anal Methods 2013;12:125–8.
[5] Liu H, Wan X, Gu L, Liu T, Yao Y. Easily accessible ferric ion chemosensor based on rhodamine derivative and its reversible OFF-ON fluorescence response. Tetrahedron 2014;70:7527–33.
[6] Sareen D, Kaur P, Singh K. Strategies in detection of metal ions using dyes. Coord Chem Rev 2014;265:125–54.
[7] Brown G, de Silva A, James M, McKinney B, Pears D, Weir S. Solid-bound, proton-driven, fluorescent 'off–on–off' switches based on PET (photoinduced electron transfer). Tetrahedron 2008;64:8301–6.
[8] Li X, Gao X, Shi W, Ma H. Design strategies for water-soluble small molecular chromogenic and fluorogenic probes. Chem Rev 2014;114:590–659.
[9] Wu Y, Zhang X, Li J, Zhang C, Liang H, Mao G, et al. Bispyrene-fluorescein hybrid based FRET cassette: a convenient platform toward ratiometric time-resolved probe for bioanalytical applications. Anal Chem 2014;86:10389–96.
[10] Bojinov V, Simeonov D, Georgiev N. A novel blue fluorescent 4-(1,2,2,6,6-pentamethylpiperidin-4-yloxy)-1,8-naphthalimide pH chemosensor based on photoinduced electron transfer. Dyes Pigments 2008;76:41–6.
[11] Jin W, Jiang J, Wang X, Zhu X, Wang G, Song Y, et al. Continuous intra-arterialblood pH monitoring in rabbits with acid-base disorders. Respir Physiol Neurobiol 2011;177:183–8.
[12] Grant S, Bettencourt K, Krulevitch P, Hamilton J, Glass R. In vitro and in vivo measurements of fiber optic and electrochemical sensors to monitor brain tissue pH. Sensors Actuators B: Chem 2001;72:174–9.
[13] Bojinov V, Panova I, Chovelon J-M. Novel blue emitting tetra- and pentamethylpiperidin-4-yloxy-1,8-naphthalimides as photoinduced electron transfer based sensors for transition metal ions and protons. Sensors Actuators B: Chem 2008;135:172–80.
[14] Young O, Thomson R, Merhtens V, Loeffen M. Industrial application to cattle of a method for the early determination of meat ultimate pH. Meat Sci 2004;67:107–12.
[15] Zhang X, Jiang H, Jin J, Xu X, Zhang Q. Analysis of acid rain patterns in northeastern China using a decision tree method. Atmos Environ 2012;46:590–6.
[16] Bojinov V, Konstantinova T. Fluorescent 4-(2,2,6,6-tetramethylpiperidin-4-ylamino)-1,8-naphthalimide pH chemosensor based on photoinduced electron transfer. Sensors Actuators B: Chem 2007;123:869–76.
[17] Lv H-S, Liu J, Zhao J, Zhao B-X, Miao J-Y. Highly selective and sensitive pH-responsive fluorescent probe in living hela and HUVEC cells. Sensors Actuators B: Chem 2013;177:956–63.
[18] Hu J, Wu F, Feng S, Xu J, Xu Z, Chen Y, et al. A convenient ratiomeric pH probe and its application for monitoring pH change in living cells. Sensors Actuators B: Chem 2014;196:194–202.
[19] Ozlem S, Akkaya E. Thinking outside the silicon box: molecular AND logic as an additional layer of selectivity in singlet oxygen generation for photodynamic therapy. J Am Chem Soc 2009;131:48–9.
[20] Zhu S, Lin W, Yuan L. Development of a ratiometric fluorescent pH probe for cell imaging based on a coumarin-quinoline platform. Dyes Pigments 2013;99:465–71.
[21] Ahamed B, Ghosh P. An integrated system of pyrene and Rhodamine-6G for selective colorimetric and fluorometric sensing of Mercury(II). Inorg Chim Acta 2011;372:100–7.
[22] Mandal A, Suresh M, Das P, Suresh E, Baidya M, Ghosh S, et al. Recognition of $Hg^{2+}$ ion through restricted imine isomerization: Crystallographic evidence and imaging in live cells. Org Lett 2012;14:2980–3.
[23] Patrick L. Mercury toxicity and antioxidants: Part 1: role of glutathione and alpha-lipoic acid in the treatment of mercury toxicity. Altern Med Rev 2002;7:456–71.
[24] Grandjean P, Weihe P, White R, Debes F. Cognitive performance of children prenatally exposed to "safe" levels of methylmercury. Environ Res 1998;77:165–72.
[25] Liu Y, Lv X, Zhao Y, Chen M, Liu J, Wang P, et al. A naphthalimide-rhodamine ratiometric fluorescent probe for $Hg^{2+}$ based on fluorescence resonance energy transfer. Dyes Pigments 2012;92:909–15.
[26] Soh J, Swamy K, Kim S, Kim S, Lee S, Yoon J. Rhodamine urea derivatives as fluorescent chemosensors for $Hg^{2+}$. Tetrahedron Lett 2007;48:5966–9.
[27] Georgiev N, Asiri A, Qusti A, Alamry K, Bojinov V. A pH sensitive and selective ratiometric PAMAM wavelength-shifting bichromophoric system based on PET, FRET and ICT. Dyes Pigments 2014;102:35–45.
[28] Ma QJ, Zhang X, Zhao X, Jin Z, Mao G, Shen G, et al. A highly selective fluorescent probe for $Hg^{2+}$ based on a rhodamine-coumarin conjugate. Anal Chim Acta 2010;663:85–90.
[29] Kim S, Swamy K, Chung S, Kim H, Kim M, Jeong Y, et al. New fluorescent and colorimetric chemosensors based on the rhodamine and boronic acid groups for the detection of $Hg^{2+}$. Tetrahedron Lett 2010;51:3286–9.
[30] Saleem M, Abdullah R, Ali A, Park B, Choi E, Hong I, et al. Synthesis, cytotoxicity and bioimaging of novel $Hg^{2+}$ selective fluorogenic chemosensor. Anal Methods 2014;6:3588–97.
[31] Alamry K, Georgiev N, Abdullah El-Daly S, Taib L, Bojinov V. A ratiometric rhodamine-naphthalimide pH selective probe built on the basis of a PAMAM light-harvesting architecture. J Lumin 2015;158:50–9.
[32] Hamilton G, Fullerton L, McCaughan B, Donnelly R, Callan J. A ratiometric fluorescent hydrogel sensor for zinc(II) based on a two fluorophore approach. New J Chem 2014;38:2823–30.
[33] Zhou J, Fang C, Chang T, Liu X, Shangguan D. A pH sensitive ratiometric fluorophore and its application for monitoring the intracellular and extracellular pHs simultaneously. J Mater Chem B 2013;1:661–7.
[34] Georgiev N, Bojinov V, Venkova A. Design, synthesis and pH sensing properties of novel PAMAM light-harvesting dendrons based on Rhodamine 6G and 1,8-naphthalimide. J Fluoresc 2013;23:459–71.
[35] Cui L, Zhu W, Xu Y, Qian X. A novel ratiometric sensor for the fast detection of palladium species with large red-shift and high resolution both in aqueous solution and solid state. Anal Chim Acta 2013;786:139–45.
[36] Georgiev N, Dimov S, Asiri A, Alamry K, Obaid A, Bojinov V. Synthesis, selective pH-sensing activity and logic behavior of highly water-soluble 1,8-naphthalimide and dihydroimidazonaphthalimide derivatives. J Lumin 2014;149:325–32.
[37] Georgiev N, Asiri A, Qusti A, Alamry K, Bojinov V. Design and synthesis of pH-selective fluorescence sensing PAMAM light-harvesting dendrons based on 1,8-naphthalimides. Sensors Actuators B: Chem 2014;190:185–98.

[38] Andréasson J, Pischel U. Smart molecules at work-mimicking advanced logic operations. Chem Soc Rev 2010;39:174–88.
[39] de Silva A, McClenaghan N. Molecular-scale logic gates. Chem Eur J 2004;10:574–86.
[40] Bojinov V, Georgiev N. Molecular sensors and molecular logic gates. J Univ Chem Tech Metall 2011;46:3–26.
[41] Andréasson J, Straight S, Kodis G, Park CD, Hambourger M, Gervaldo M, et al. All-photonic molecular half-adder. J Am Chem Soc 2006;128:16259–65.
[42] Georgiev N, Lyulev M, Bojinov V. Sensor activity and logic behaviour of PET based dihydroimidazonaphthalimide diester. Spectrochim Acta Part A 2012;97:512–20.
[43] Margulies D, Melman G, Shanzer A. A molecular full-adder and full-subtractor, an additional step toward a moleculator. J Am Chem Soc 2006;128:4865–71.
[44] Li Q, Yue Y, Guo Y, Shao S. Fluoride anions triggered "OFF–ON" fluorescent sensor for hydrogen sulfate anions based on a BODIPY scaffold that works as a molecular keypad lock. Sensors Actuators B: Chem 2012;173:797–801.
[45] Suresh M, Jose D, Das A. [2,2′-Bipyridyl]-3,3′-diol as a molecular half-subtractor. Org Lett 2007;9:441–4.
[46] Ceroni P, Bergamini G, Balzani V. Old molecules, new concepts: $[Ru(bpy)3]^{2+}$ as a molecular encoder-decoder. Angew Chem Int Ed 2009;48:8516–8.
[47] Georgiev N, Lyulev M, Alamry K, Abdullah El-Daly S, Taib L, Bojinov V. Synthesis, sensor activity and logic behavior of a highly water-soluble 9,10-dihydro-7H-imidazo[1,2-*b*]benz[*d*,*e*]isoqionolin-7-one dicarboxylic acid. J Photochem Photobiol A: Chem 2014;297:31–8.
[48] Jiang W, Zhang H, Liu Y. Unimolecular half-adders and half-subtractors based on acid-base reaction. Front Chem China 2009;4:292–8.
[49] Georgiev N, Yaneva I, Surleva A, Asiri A, Bojinov V. Synthesis, selective pH-sensing activity and logic behavior of highly water-soluble 1,8-naphthalimide and dihydroimidazonaphthalimide derivatives. Sensors Actuators B: Chem 2013;184:54–63.
[50] Macdonald J, Li Y, Sutovic M, Lederman H, Pendri K, Lu W, et al. Medium scale integration of molecular logic gates in an automaton. Nano Lett 2006;6:2598–603.
[51] Pais V, Remon P, Collado D, Andréasson J, Perez-Inestrosa E, Pischel U. OFF-ON-OFF fluorescence switch with T-latch function. Org Lett 2011;13:5572–5.
[52] Pu F, Ju E, Ren J, Qu X. Multiconfigurable logic gates based on fluorescence switching in adaptive coordination polymer nanoparticles. Adv Mater 2014;26:1111–7.
[53] Bojinov V, Venkova A, Georgiev N. Synthesis and energy-transfer properties of fluorescence sensing bichromophoric system based on Rhodamine 6G and 1,8-naphthalimide. Sensors Actuators B: Chem 2009;143:42–9.
[54] Kubin R, Fletcher A. Fluorescence quantum yields of some rhodamine dyes. J Lumin 1982;27:455–62.
[55] Reynolds G, Drexhage K. New coumarin dyes with rigidized structure for flashlamp-pumped dye lasers. Opt Commun 1975;13:222–5.
[56] Adronov A, Malenfant P, Frechet J. Synthesis and steady-state photophysical properties of dye-labeled dendrimers having novel oligothiophene cores: A comparative study. Chem Mater 2000;12:1463–72.
[57] Georgiev N, Asiri A, Alamry K, Obaid A, Bojinov V. Selective ratiometric pH-sensing PAMAM light-harvesting dendrimer based on Rhodamine 6G and 1,8-naphthalimide. J Photochem Photobiol A: Chem 2014;277:62–74.
[58] Alamry K, Georgiev N, El-Daly S, Taib L, Bojinov V. A highly selective ratiometric fluorescent pH probe based on a PAMAM wavelength-shifting bichromophoric system. Spectrochim Acta Part A 2015;135:792–800.
[59] Bojinov V, Georgiev N, Nikolov P. Synthesis and photophysical properties of fluorescence sensing ester- and amidoamine-functionalized 1,8-naphthalimides. J Photochem Photobiol A: Chem 2008;193:129–38.
[60] Georgiev N, Sakr A, Bojinov V. Design and synthesis of novel fluorescence sensing perylene diimides based on photoinduced electron transfer. Dyes Pigments 2011;91:332–9.
[61] Gunnlaugsson T, McCoy C, Morrow R, Phelan C, Stomeo F. Towards the development of controllable and reversible "on-off' luminescence switching in soft-matter; synthesis and spectroscopic investigation of 1,8-naphthalimidebased PET (photoinduced electron transfer) chemosensors for pH in waterpermeable hydrogels. ARKIVOC 2003;VII:216–28.
[62] Georgiev N, Bojinov V. The design and synthesis of a novel 1,8-naphthalimide PAMAM light-harvesting dendron with fluorescence "off-on" switching core. Dyes Pigments 2010;84:249–56.
[63] Georgiev N, Bojinov V, Nikolov P. Design, synthesis and photophysical properties of two novel 1,8-naphthalimide fluorescent pH sensors based on PET and ICT. Dyes Pigments 2011;88:350–7.
[64] Daffy L, de Silva AP, Gunaratne H, Huber C, Lynch P, Werner T, et al. Arene-dicarboximide building blocks for fluorescent photoinduced electron transfer pH sensors applicable with different media and communication wavelengths. Chem Eur J 1998;4:1810–5.
[65] Wang R, Yu C, Yu F, Chen L. Molecular fluorescent probes for monitoring pH changes in living cells. Trends Anal Chem 2010;29:1004–13.
[66] Bojinov V, Georgiev N, Bosch P. Design and synthesis of highly photostable yellow-green emitting 1,8-naphthalimides as fluorescent sensors for metal cations and protons. J Fluoresc 2009;19:127–39.
[67] Attia M, Youssef A, El-Sherif R. Durable diagnosis of seminal vesicle and sexual gland diseases using the nano optical sensor thin film Sm-doxycycline complex. Anal Chim Acta 2014;835:56–64.
[68] Lee M, Lee S, Jung J, Lima H, Kim J. Luminophore-immobilized mesoporous silica for selective $Hg^{2+}$ sensing. Tetrahedron 2007;63:12087–92.
[69] Luo J, Jiang S, Qin S, Wu H, Wang Y, Jiang J, et al. Highly sensitive and selective turn-on fluorescent chemosensor for $Hg^{2+}$ in pure water based on a rhodamine containing water-soluble copolymer. Sensors Actuators B: Chem 2011;160:1191–7.
[70] de Silva A. Molecular logic-based computation. Cambridge: Royal Society of Chemistry; 2013.